ADVANCED OPTICAL MATERIALS

Supporting Information

for *Adv. Optical Mater.,* DOI: 10.1002/adom.202001923

Self-Assembled Plasmonic Coaxial Nanocavities for High-Definition Broad-Angle Coloring in Reflection and Transmission

Haibin Ni, Alexey V. Krasavin, Lu Zhang, An Ping, Chao Pan, Jianxin Cheng, Ming Wang, Jianhua Chang,* and Anatoly V. Zayats**

Supporting Information

Self-Assembled Plasmonic Coaxial Nanocavities for High-Definition Broad-Angle Coloring in Reflection and Transmission

Haibin Ni,[1,] Alexey V. Krasavin,[2] Lu Zhang,[1] An Ping,[1] Chao Pan,[1] Jianxin Cheng,[1] Ming Wang,[3] Jianhua Chang,[1*] and Anatoly. V. Zayats[2*]*

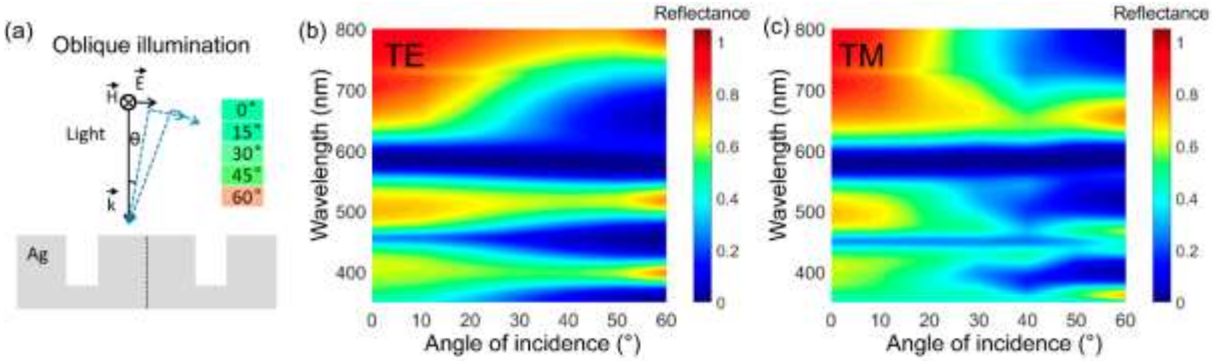

Figure S1. a) Schematics of the oblique illumination of the coaxial nanocavity and the corresponding reflection colors at various angles of incidence. b–c) Simulated reflection spectra as a function of the incident angle for (b) TE- and (c) TM-polarized light impinging the coaxial nanocavity array with geometrical parameters of R = 50 nm, W = 20 nm, H = 150 nm, and P = 250 nm.

Complementing the experimental measurements, angle resolved reflection spectra and the corresponding encoded colors were investigated numerically varying the angle of incidence from 0° to 60° for both TE and TM polarizations (Figure S1 b–c). Similarly to the experimental results, the main reflection dips (in this case designed to reproduce a green color) keep their spectral positions experiencing some broadening, while additional modes at the edges of the visible spectrum appear above 30° illumination/observation. At the same time, the reproduced color shows high robustness to these changes, being pure green up to 45°.

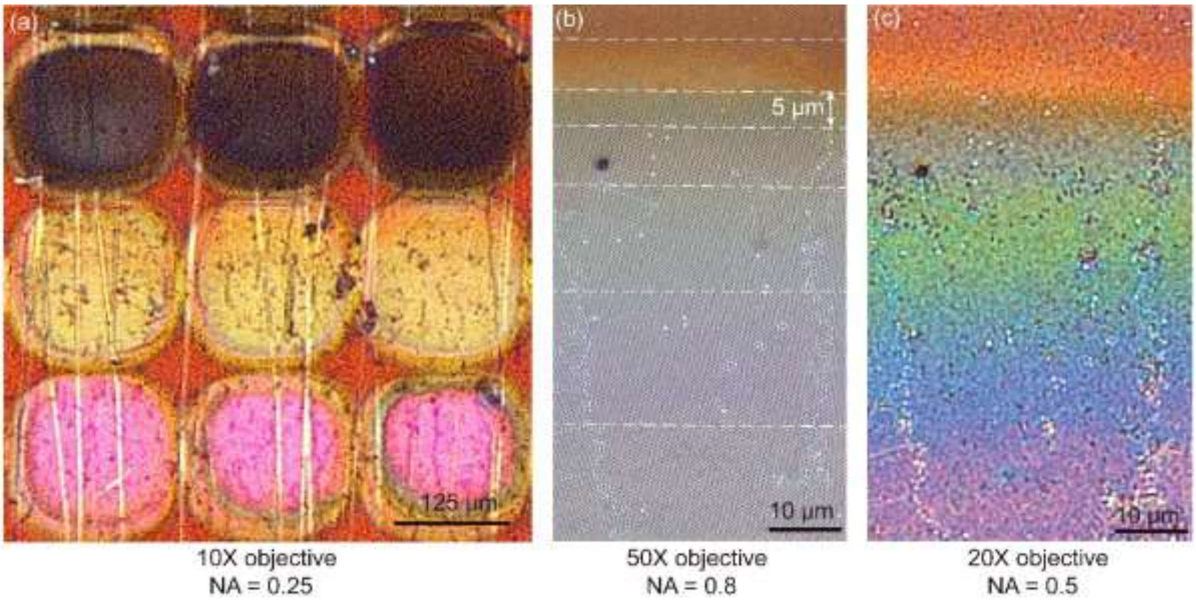

Figure S2. a) Pixel arrays of various colours achieved using mask-assisted RIE. b) High-resolution reflection image revealing the size of individual nanostructures which are individual color pixels (NA = 0.8, P = 690 nm, R ~ 150 nm, W ~ 60 nm, and H varied in the range ~ 180–380 nm from bottom to top; dashed lines separate the pixel arrays with different W). The colors are difficult to distinguish because of the low brightness due to the use of a high-NA objective. c) The same area as in (b) observed with a NA = 0.5 objective which provides higher brightness but smaller resolution. Color variations are clearly seen for pixels due to the gradient in Ar RIE milling.

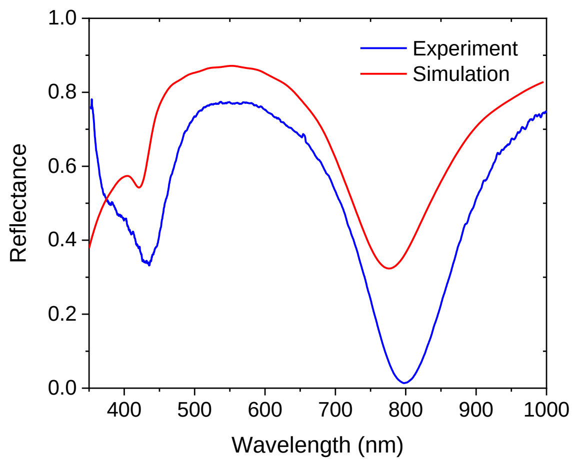

Figure S3. Experimental and simulated reflectance spectra of the coaxial cavities with R = 105 nm, W = 12 nm, H = 100 nm and P = 250 nm.

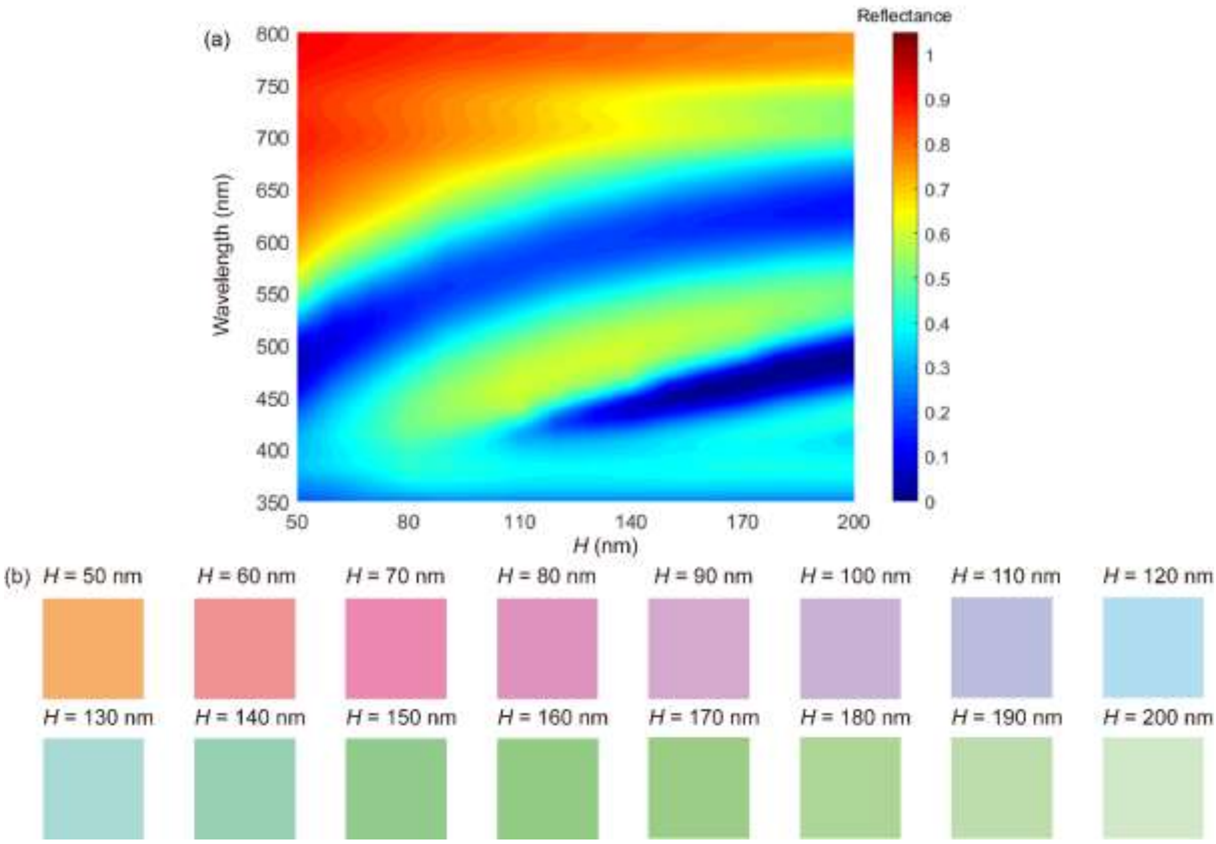

Figure S4. a) Simulated reflectance spectra and b) corresponding colors of the coaxial cavity arrays with P = 200 nm, R = 40 nm, W = 20 nm and H varied from 50 nm to 200 nm. When the height reaches H = 170 nm the spectrum results in a green color.

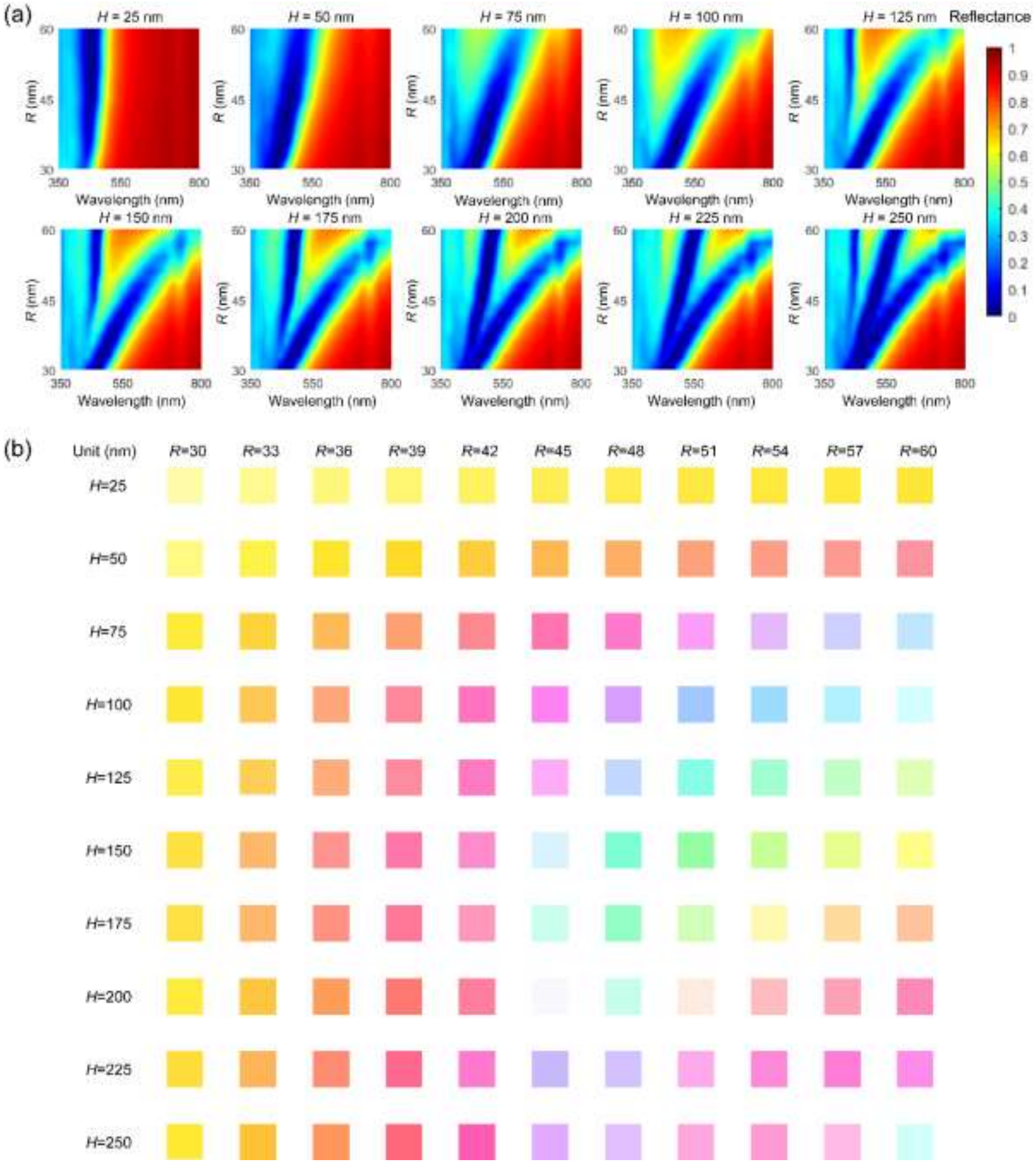

Figure S5. a) Simulated reflectance spectra and b) corresponding colors of the coaxial cavity arrays with P = 150 nm, W = 20 nm, and H and R varied from 25 nm to 250 nm and from 30 nm to 60 nm, respectively.